THE JOURNAL OF BIOLOGICAL CHEMISTRY VOL. 281, NO. 17, pp. 11618–11626, April 28, 2006
Printed in the U.S.A.

Quaternary Structure and Cleavage Specificity of a Poxvirus Holliday Junction Resolvase*

Received for publication, January 9, 2006, and in revised form, February 21, 2006 Published, JBC Papers in Press, March 2, 2006, DOI 10.1074/jbc.M600182200

Alonzo D. Garcia[‡1], Joel Otero[‡2], Jacob Lebowitz[§], Peter Schuck[§], and Bernard Moss[‡3]

From the [‡]Laboratory of Viral Diseases, NIAID and the [§]Division of Bioengineering and Physical Science, Office of Research Services, National Institutes of Health, Bethesda, Maryland 20892

Recently, poxviruses were found to encode a protein with signature motifs present in the RuvC family of Holliday junction (HJ) resolvases, which have a key role in homologous recombination in bacteria. The vaccinia virus homolog A22 specifically cleaved synthetic HJ DNA *in vitro* and was required for the *in vivo* resolution of viral DNA concatemers into unit-length genomes with hairpin telomeres. It was of interest to further characterize a poxvirus resolvase in view of the low sequence similarity with RuvC, the absence of virus-encoded RuvA and RuvB to interact with, and the different functions of the viral and bacterial resolvases. Because purified A22 aggregated severely, studies were carried out with maltose-binding protein fused to A22 as well as to RuvC. Using gel filtration, chemical cross-linking, analytical ultracentrifugation, and light scattering, we demonstrated that A22 and RuvC are homodimers in solution. Furthermore, the dimeric form of the resolvase associated with HJ DNA, presumably facilitating the symmetrical cleavage of such structures. Like RuvC, A22 symmetrically cleaved fixed HJ junctions as well as junctions allowing strand mobility. Unlike RuvC and other members of the family, however, the poxvirus enzyme exhibited little cleavage sequence specificity. Structural and enzymatic similarities of poxvirus, bacterial, and fungal mitochondrial HJ resolvases are consistent with their predicted evolutionary relationship based on sequence analysis. The absence of a homologous resolvase in mammalian cells makes these microbial enzymes excellent potential therapeutic targets.

Poxviruses, of which vaccinia virus (VACV)[4] is the prototype, replicate in the cytoplasm of cells and encode enzymes for DNA and RNA synthesis (1). The genome of poxviruses consists of a linear double-stranded DNA molecule with the ends of each strand covalently linked to the other by incompletely base-paired hairpins, thus forming a continuous polynucleotide chain (2). The hairpins form following DNA replication during the resolution of long concatemers into unit length genomes (3, 4). When transfected into infected cells, circular plasmids containing the concatemer junction are resolved into minigenomes with covalently closed hairpin ends by a conservative strand exchange mechanism (5–7). The concatemer junction contains an inverted repetition, which in supercoiled plasmids can form a cruciform structure resembling a four-way Holliday junction (HJ) recombination intermediate (8, 9). HJ resolving enzymes have been isolated from many organisms and can be divided into two main functional groups (10). Members of the first group, which have *Escherichia coli* RuvC as the prototype, have been isolated from bacteria, Archaea, and yeast. These endonucleases have high selectivity for the HJ, exhibit some sequence specificity for cleavage, and are thought to have roles in DNA recombination and repair. The second functional group, which are encoded by bacteriophages, cleave a variety of branched DNAs, exhibit low sequence specificity, and have roles in repairing double strand breaks, recombination, and processing of DNA before packaging.

Studies with VACV mutants and cell extracts suggested that a virus-encoded late protein is required for resolution of concatemers (11–13) and two candidate proteins have been considered. The VACV-encoded type 1 topoisomerase (14, 15) cleaves and ligates a variety of DNA structures including a HJ (16, 17). Nevertheless, viral DNA concatemers are resolved into unit length genomes in cells infected with a VACV topoisomerase deletion mutant and a role for the enzyme in enhancing early gene expression within the confines of the virus core was suggested (18). The other candidate resolving enzyme was identified by reiterative PSI-BLAST searches, which led to the finding of 5 motifs or structural elements that are critical for activity of *E. coli* RuvC in an open reading frame (ORF) that is conserved in all poxvirus genomes, a distantly related iridovirus, and yeast (19, 20). A recombinant form of the poxvirus RuvC homolog encoded by the A22R ORF of VACV was shown to specifically bind and cleave a synthetic HJ to yield a nicked duplex molecule (19). Mutation of either of two conserved acidic amino acids abrogated the catalytic activity of the viral protein without affecting HJ binding (19). Furthermore, a VACV-inducible A22 mutant was defective in processing concatemers into unit-length genomes with hairpin ends under non-permissive conditions (21). Thus, the HJ resolvase activity of the A22 protein is likely to be directly involved in concatemer resolution, though the enzyme may have additional roles in DNA replication and processing. Thus far, resolvase activity of RuvC homologs of other poxviruses or iridoviruses has not been confirmed, although the conservation of critical amino acid residues makes such activity likely. The presence of homologs of RuvC in bacteria, yeast, and poxviruses and their absence in mammals suggest that these enzymes are prime targets for antimicrobial therapy.

E. coli RuvC has been extensively characterized with regard to both catalytic activity and atomic structure. The 19-kDa protein has been shown to be dimeric by gel filtration and x-ray crystallography (22, 23). The binding of a RuvC dimer to a HJ ensures that nicks will be introduced symmetrically and simultaneously or nearly so into the two homologous strands. In addition, RuvC exhibits specificity for cleaving at specific nucleotide sequences (24, 25). Here we provide evidence that the VACV A22 protein is a dimer in solution and when bound to HJ

* This research was supported in part by the Intramural Research Program of NIAID, National Institutes of Health. The costs of publication of this article were defrayed in part by the payment of page charges. This article must therefore be hereby marked "*advertisement*" in accordance with 18 U.S.C. Section 1734 solely to indicate this fact.

[1] Present address: Laboratory of DNA Viruses, Division of Viral Products, HFM-457, Center for Biologics Evaluation and Research, Food and Drug Administration, 1401 Rockville Pike, Rockville, Bethesda, MD 20892.

[2] Present address: Cell and Molecular Biology Program, Baylor College of Medicine, One Baylor Plaza, Rm. N1130, Houston, TX 77030.

[3] To whom correspondence should be addressed. Tel.: 301-496-9869; Fax: 301-480-1147; E-mail: bmoss@nih.gov.

[4] The abbreviations used are: VACV, vaccinia virus; MBP, maltose-binding protein; HJ, Holliday junction; DTT, dithiothreitol; ORF, open reading frame; EGS, ethylene glyco bis(succinimidyl) succinate.

structures. In addition, the sequence specificity of cleavage by A22 was investigated and found to differ from that of RuvC.

EXPERIMENTAL PROCEDURES

Recombinant A22 and RuvC

Construction of Plasmids Encoding A22 and RuvC Fused to the C Terminus of the Maltose-binding Protein (MBP)—The A22R ORF was amplified by polymerase chain reaction (PCR) using oligonucleotide primers 5′-GGGCGATATCGAAACTTTAACCAGTTCGTCTCAATC and 5′-GGGGGGATCCTTAGTGATGGTGATGGTGATGCATTTTTTTTTATGTAATTTCTAGATTTAC (EcoRV and BamHI sites underlined). The PCR product was purified and ligated into pCR2.1-TOPO TA-cloning vector (Invitrogen) resulting in pCR2.1-A22R. An EcoRV-BamHI fragment was excised from pCR2.1-A22R, gel-purified, and ligated to XmnI and BamHI cut pMAL-c2 vector (New England Biolabs) creating pMAL-A22R. A similar PCR protocol was used to amplify the RuvC ORF using genomic DNA purified from *E. coli* strain DH5 lysate and oligonucleotide primers 5′-GGGCGGATATCGCTATTATTCTCGGCATTGATCCGGG and 5′GGGGGGATCCTTAACGCAGTCGCCCTCTCGCCAGGTTCAGCC (EcoRV and BamHI sites underlined). The PCR product was purified and inserted into pCR2.1-TOPO TA-cloning vector resulting in pCR2.1-RuvC. An EcoRV-BamHI fragment containing the RuvC ORF from pCR2.1-RuvC was cloned into pMAL-c2 vector, as described above, creating pMAL-RuvC. *E. coli* strain DH5 (New England Biolabs) was transformed for plasmid amplification.

Expression of MBP-A22 and MBP-RuvC—*E. coli* strain ER2508 (New England Biolabs), which is deficient in the lon protease and MBP, was transformed with pMAL-A22R and pMAL-RuvC to express MBP-A22 and MBP-RuvC, respectively. Cells were typically grown to an A_{600} of 0.5 in 1 liter of LB-broth containing 0.2% (w/v) glucose and 100 μg of ampicillin per ml. Expression of fusion proteins was induced by adding isopropyl-β-D-thiogalactopyranoside to a final concentration of 0.3 mM. After 3 h, the cells were harvested by centrifugation, and the pellet was frozen and resuspended in MBP buffer (25 mM Tris-HCl, pH 7.5, 200 mM NaCl, 1 mM EDTA, 1 mM DTT, 0.2 mM phenylmethylsulfonyl fluoride) plus Complete, EDTA-free Protease Inhibitor Mixture tablets (Roche Applied Science). The cells were lysed by sonication (eight 15-s bursts on ice), and the lysate was centrifuged at 9,000 × *g* for 30 min. The clarified bacterial extract (50 ml) was diluted by adding four volumes of MBP column buffer containing 0.2 mM phenylmethylsulfonyl fluoride and passed through an amylose affinity column (New England Biolabs) previously equilibrated with MBP buffer. After the column was washed with 12-column volumes of MBP buffer, the recombinant protein was eluted with MBP buffer containing 10 mM maltose, and 1-ml fractions were collected. Fractions were analyzed by SDS-polyacrylamide gel electrophoresis (PAGE) and stained with Coomassie Blue. The peak protein fractions were pooled, 10% glycerol final concentration was added, and the protein concentration was determined.

Physical Analysis of A22

Gel Filtration—A HiPrep 16/60 S-300 Sephacryl HR column (Amersham Biosciences) was equilibrated with buffer A (25 mM Tris-HCl, pH 7.5, 1 mM DTT, 1 mM EDTA, 10% (v/v) glycerol) containing 0.2 M or 0.8 M NaCl. The column was calibrated with molecular weight (MW) standards (Amersham Biosciences) blue dextran 2000 (MW 2.0 × 10^6), ferritin (MW 440,000), aldolase (MW 158,000), bovine serum albumin (MW 67,000), and chymotrypsinogen A (MW 25,000). Affinity-purified MBP-A22 or MBP-RuvC (1 to 2 mg) was applied to the gel filtration column. Protein fractions were collected and analyzed on a 4–20% SDS-polyacrylamide gel and detected with silver staining reagents (Owl).

Chemical Cross-linking—Affinity-purified MBP-A22 (1.5 mg) and MBP-RuvC (2.0 mg) were further purified by gel filtration on a HiPrep 16/60 S-300 Sephacryl HR column that had been equilibrated with buffer B (20 mM HEPES-HCl pH 7.5, 800 mM NaCl, 1 mM DTT, 1 mM EDTA) and calibrated as described above. MBP-A22 and MBP-RuvC peak fractions corresponding to ~130,000 kDa were combined with various concentrations of EGS. A final concentration of ~0.4 μg/μl of MBP-A22 or MBP-RuvC was incubated in 20-μl reactions at room temperature for 30 min. Reactions were quenched with glycine at a final concentration of 100 mM. Cross-linked products were analyzed by Western blotting.

Analytical Ultracentrifugation—Sedimentation velocity experiments were conducted in an Optima XLI/A (Beckman Coulter, Fullerton, CA). From 350 to 400 μl of protein at concentrations of 50–400 μg/ml in buffered 0.8 M NaCl were filled in double sector centerpieces and interference fringe displacement data were acquired in time intervals of 100 s at a rotor speed of 50,000 rev/min and a temperature of 20 °C. Protein partial-specific volumes and buffer density and viscosity were estimated with the software SEDNTERP, kindly provided by Dr. J. Philo (Alliance Protein Laboratories, Thousand Oaks, CA). Data were analyzed by direct boundary modeling with the software SEDFIT, using the model for the continuous sedimentation coefficient distribution c(s) with maximum entropy regularization (26), combined with a discrete species describing the redistribution of unmatched buffer components and with algebraic elimination of the systematic noise components (27). After determining the best-fit weight-average frictional ratio of the protein components, the c(s) distribution was transformed into the corresponding molar mass distribution c(M) (28). Alternatively, a boundary model with discrete Lamm equation solutions was fitted globally to data sets at different loading concentrations, using the software SEDPHAT. With both methods, the final root mean square errors of the fit were generally below 0.005 fringes.

On-line Size Exclusion Chromatography Multi-angle Laser Light Scattering—An Amersham Biosciences Superdex HR200 column was used for the size exclusion separation of protein components. The flow rates used for MBP-RuvC were 0.65–0.7 ml/min, and 50–200 μl of 0.80 mg/ml protein were injected into the column. The flow rate for MBP-A22 was 0.35 ml/min, and 200 μl of 0.65 mg/ml was injected into the column. The eluant from the column entered the UV detector (Waters 2487) followed by the multi-angle light scattering detector (Wyatt Technology Dawn EOS). Wyatt Technology Astra software was used for the data analysis, and the molar mass was determined as described (29). A correction factor of 1.23 (based on the molar mass determination in phosphate-buffered saline relative to the resolvase buffer) was applied to correct for the high refractive index of the resolvase buffer.

Mobility Shift Assay—DNA binding reactions were performed in a volume of 20 μl containing rA22-his (19) or MBP-A22 (uncleaved or partially cleaved with Factor Xa protease), 0.01 pmol of ^{32}P-labeled HJ-1, 20 mM Tris-HCl (pH 8.0), 1 mM DTT, 100 μg/ml bovine serum albumin, 5% glycerol, 50 mM NaCl, and 1 mM EDTA. DNA binding reactions were incubated for 20 min at room temperature. Afterward, a loading dye solution was added to give the final concentrations of 20 mM HEPES-HCl (pH 7.5), 5% glycerol, and 0.02% bromphenol blue. Bound and unbound HJ probes were separated by electrophoresis through a 4% (30:1, acrylamide to bis acrylamide) polyacrylamide gel containing 0.5× TBE (89 mM Tris borate, 2 mM EDTA, pH 8.3). Electrophoresis was performed at 4 °C at ~150 volts until bromphenol blue migrated close

to the bottom of the gel. The gel was dried on Whatman DE-81 paper, and bands were visualized by autoradiography.

Factor Xa Protease Cleavage—Reactions contained 200 ng/μl of MBP-A22, 0.05 ng/μl of Factor Xa (New England Biolabs), 20 mM Tris-HCl (pH 7.5), 200 mM NaCl, 1 mM EDTA, and 10 mM β-mercaptoethanol. After 2–4 h at room temperature, the mixtures were kept on ice until used.

Preparation of Synthetic HJs

HJ-1—The following oligonucleotides were annealed to make an HJ with a 2-bp region of homology (underlined nucleotides) as previously described (30). HJ-1, 5′-GGTAGGACGGCCTCGCAATCGGCTTTGACCGAGCACGCGAGATGTCAACG; HJ-2, 5′-CGTTGACATCTCGCGTGCTCGGTCAATCGGCAGATGCGGAGTGAAGTTCC; HJ-3, 5′-GGAACTTCACTCCGCATCTGCCGATTCTGGCTGTGGCGTGTTTCTGGTGG; HJ-4, 5′-CCACCAGAAACACGCCACAGCCAGAAAGCCGATTGCGAGGCCGTCCTACC.

HJ-bm4—The following oligonucleotides were annealed to make a HJ with a 12-bp region of homology (underlined nucleotides). The oligonucleotides were similar to those previously described (31) except that 10 nucleotides were added to the 5′- and 3′-ends to increase the length to 50 nucleotides. bm4-1, 5′-CCACCAGAAAGGAATCATCCACTCGCCTTAACACTGCGTTCCGTCCTACC; bm4-2, 5′-GGTAGGACGGAACGCAGTGTTAAGGCGAGTGATCCAGGTTGATGTCAACG; bm4-3, 5′-CGTTGACATCAACCTGGATCACTCGCCTTAATCGCTGCGGTGAAGTTCC; bm4-4, 5′-GGAACTTCACCGCAAGCGATTAAGGCGAGTGGATGATTCCTTTCTGGTGG.

HJ-X12—The following oligonucleotides were annealed to make a HJ that contains a 12-bp region of homology (underlined nucleotides) as previously described (32). X12-1, 5′-GACGCTGCCGAATTCTGGCTTGCTAGGACATCTTTGCCCACGTTGACCCA; X12-2, 5′-TGGGTCAACGTGGGCAAAGATGTCCTAGCAATGTAATCGTCTATGACGTT; X12-3, 5′-AACGTCATAGACGATTACATTGCTAGGACATGCTGTCTAGAGACTATCGA; X12-4, 5′-TCGATAGTCTCTAGACAGCATGTCCTAGCAAGCCAGAATTCGGCAGCGTC.

Jun3—The following oligonucleotides were annealed to make a static Holliday junction as previously described (31). Jun3-1, 5′-CCTCGAGGGATCCGTCCTAGCAAGGGGCTGCTACCGGAAGCTTCTCGAGG; Jun3-2, 5′-CCTCGAGAAGCTTCCGGTAGCAGCCTGAGCGGTGGTTGAATTCCTCGAGG; Jun3-3, 5′-CCTCGAGGAATTCAACCACCGCTCAACTCAACTGCAGTCTAGACTCGAGG; Jun 3-4, 5′-CCTCGAGTCTAGACTGCAGTTGAGTCCTTGCTAGGACGGATCCCTCGAGG.

Oligonucleotides used to make HJ substrates were gel-purified by electrophoresis through a 12% (20:1, acrylamide to bisacrylamide) polyacrylamide gel containing 8.3 M urea in 1× TBE. Bands were visualized by UV illumination, excised, and oligonucleotides were extracted by soaking minced gel slices in 4 ml of TE buffer (10 mM Tris, 1 mM EDTA, pH 8.0) overnight at 37 °C with continuous shaking. Oligonucleotides were purified and concentrated using Sep-Pak® C18 cartridges (Waters), dried and resuspended in H_20. Prior to annealing, oligonucleotides were 5′-^{32}P end-labeled using T4 polynucleotide kinase and [γ-^{32}P]ATP (6000 Ci/mmol; 1 Ci = 1 GBq). Kinase reactions were terminated by phenol/chloroform extraction and unincorporated radiolabel was removed by passing the aqueous phase through G-50 spin microcolumn (Amersham Biosciences). The final HJ product contained one 5′-^{32}P-labeled strand and three unlabeled strands. For 5′-^{32}P-labeled HJ-bm4 and HJ-X12 substrates, annealed products were purified by electrophoresis through a 6% (20:1, acrylamide to bisacrylamide) polyacrylamide gel containing 1× TBE. Bands were excised and HJ substrates were extracted by electroelution following the manufacturer's instructions (Bio-Rad).

Holliday Junction Cleavage Assays

Affinity-purified MBP-A22 and MBP-RuvC were further purified by gel filtration as described above using buffer-A with 0.8 M NaCl, concentrated using Centricon plus-20 centrifugal filter units (Millipore), and quantified with the Bradford protein assay (Bio-Rad). Reaction mixtures of 20 μl contained ~1 pmol of 5′-^{32}P-labeled HJ, 10 pmol of MBP-A22, 20 mM Tris-HCl (pH 8.0), 0.5 mM $MgCl_2$ (determined to be optimal), 1 mM DTT, 100 μg/ml bovine serum albumin, 5% glycerol, and 50 mM NaCl. Incubations were for 20 min at 37 °C. Cleavage reactions containing 10 pmol of MBP-RuvC were done identically except that 10 mM $MgCl_2$ was used. Reactions were terminated by addition of a stop solution to give final concentrations of 0.2% SDS, 20 mM EDTA, and 0.6 μg/μl proteinase K. After incubating at 37 °C for 20 min, a sucrose loading dye solution was added to give final concentrations of 4% sucrose, 0.02% bromphenol blue, and 0.02% xylene cyanol FF. Cleavage products were evaluated by electrophoresis through a 10% (20:1, acrylamide to bisacrylamide) polyacrylamide gel containing 1× TBE, and bands were visualized by autoradiography. To map the positions of HJ cleavage, the products and sequencing ladders of HJ substrates that had been subjected to chemical cleavage (33) were resuspended in sequence loading dye (90% formamide, 10 mM EDTA, pH 8.0, 0.02% bromphenol blue, 0.02% xylene cyanol FF) and denatured by heating at 95 °C for 3 min. Cleavage products and sequencing ladders were then electrophoresed under denaturing conditions through a 12% (20:1, acrylamide to bisacrylamide) polyacrylamide gel containing 8.3 M urea in 1× TBE. Gels were then fixed, dried on Whatman 3M paper, and bands were visualized by autoradiography. A 1.5-base allowance was made to compensate for the nucleoside eliminated in the sequencing reaction.

RESULTS

Gel Filtration of MBP-A22—We previously expressed a recombinant form of the A22 protein, with six histidine residues appended to the C terminus, in *E. coli* and purified the protein by metal affinity chromatography (19). Although the protein was enzymatically active, it was highly aggregated limiting its usefulness for further characterization. To improve its physical properties, A22 was expressed as a 65-kDa polypeptide fused to the C terminus of the MBP. Previous studies showed that similar fusions of MPB with RuvC and CCE1 had no discernible effect on DNA binding or enzymatic activity (34, 35). Nevertheless, we also made the corresponding RuvC fusion protein for comparative purposes. The A22 fusion protein was purified by affinity chromatography on an amylose resin and analyzed by gel filtration on a S-300 Sephacryl HR column followed by SDS-PAGE and silver staining. The fusion protein was highly aggregated at 0.2 M NaCl and eluted in the void volume of the Sephacryl column (not shown). When the NaCl concentration was increased to 0.8 M, however, the protein disaggregated and eluted mostly between 67- and 158-kDa markers consistent with a dimer of 65-kDa polypeptides (Fig. 1*A*). As a control, we expressed and analyzed a 61-kDa MBP-RuvC fusion protein. The latter eluted from a S-300 Sephacryl column at approximately the same position as MBP-A22, except that some aggregated protein also eluted in the void volume at 0.8 M NaCl (Fig. 1*B*). The Stokes radii of MBP-A22 and MBP-RuvC were calculated to be ~42.3 Å (36).

Cross-linking of A22 Dimers—Evidence that MBP-A22 exists as a dimer was obtained by chemical cross-linking. Purified MBP-A22 and MBP-RuvC were treated with increasing amounts of EGS and analyzed

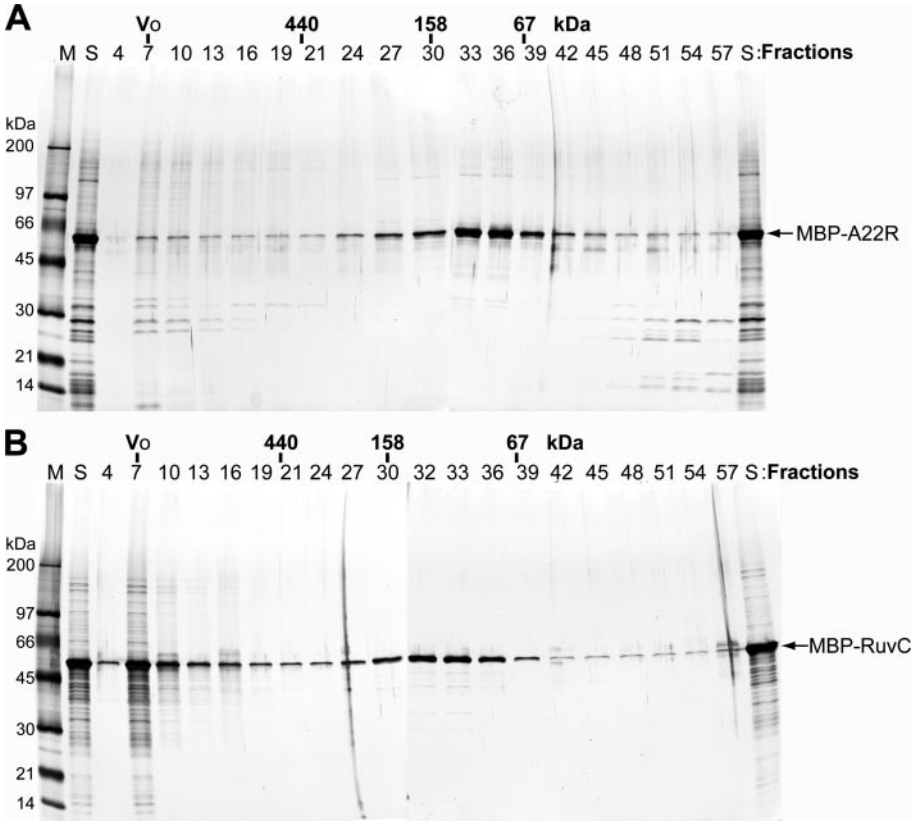

FIGURE 1. **Gel filtration.** MBP-A22 (*A*) and MBP-RuvC (*B*) fusion proteins were purified by amylose affinity chromatography in a buffer containing 0.2 M NaCl. The salt concentration was then increased to 0.8 M, and the proteins were applied to an S-300 Sephacryl HR column. Every third fraction was analyzed by SDS-PAGE and silver staining. Stained gels are shown with the lanes corresponding to marker proteins (*M*), loading sample (*S*), and numbered fractions. The column was calibrated with blue dextran 2000, which marks the void volume (V_o) and standard proteins ferritin, aldolase, bovine serum albumin, and chymotrypsinogen. Masses of marker proteins are indicated *above* their peak elution fractions. *Arrows* point to the MBP-A22 and MBP-RuvC bands.

by SDS-PAGE and Western blotting. The untreated proteins migrated as expected for monomers in the presence of SDS. In contrast, the major cross-linked species of MBP-A22 and MBP-RuvC migrated at positions expected for dimers (Fig. 2). The diminution in intensity of bands at high EGS concentrations can be explained by decreased reactivity to antibody.

Sedimentation Velocity and Light Scattering of A22 and RuvC Dimers—Sedimentation velocity and light scattering were used to further investigate the association state of A22. Sedimentation equilibrium measurements were attempted but aggregation occurred during the 2–3 days required for this procedure. Sedimentation velocity profiles for MBP-A22 in 0.8 M NaCl are shown in Fig. 3*A*. The data could be well modeled as a continuous sedimentation coefficient distribution as indicated by a plot of the residuals (Fig. 3*B*). A single peak at 5.77S was obtained, which corresponds to a molar mass distribution of 130 kDa (Fig. 3*C*, *solid line*). Sedimentation data from experiments using 0.9 and 6 μM MBP-A22 could be modeled well as discrete protein species of 115 kDa (not shown). These data indicate that MBP-A22 exists as a dimer with a shape that corresponds hydrodynamically to an ellipsoid with an axial ratio of ~7:1. Similar results were obtained for MBP-RuvC. The molar mass distribution led to an estimate of 135 kDa for MBP-RuvC (Fig. 3*C*, *dashed line*) and sedimentation data acquired at loading concentrations of 0.8 and 5 μM could be globally modeled as discrete species of 138 kDa. This indicates that MBP-RuvC is also present in solution as a dimer with a hydrodynamic friction corresponding to an ellipsoid with an axial ratio of ~8:1. The slightly higher molar mass estimates for RuvC compared with A22 was attributed to errors in the estimated buoyancy of the former protein due to preferential solvation.

For multi-angle light scattering experiments, MBP-A22 and MBP-RuvC were purified and stored in buffered 8% glycerol and 0.8 M NaCl to minimize aggregation. The size exclusion chromatography elution profile showed two very well resolved peaks, one corresponding to the dimer component and the other to aggregates (not shown). The light scattering molar mass determinations of MBP-RuvC and MBP-A22 are shown in Fig. 4, *panels A* and *B*, respectively. For MBP-A22, we observed a weight average molar mass of 132,700 compared with the theoretical dimer mass of 132,277. The weight-average molar mass of MBP-RuvC was 121,930 compared with the theoretical dimer mass of 122,400. In summary, the biophysical measurement unequivocally demonstrated both MBP-A22 and MBP-RuvC are dimeric in solution and have asymmetric shapes.

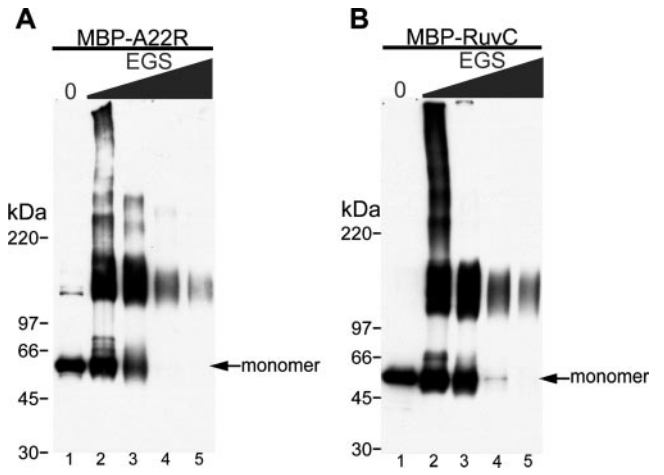

FIGURE 2. **EGS cross-linking.** MBP-A22 and MBP-RuvC fusion proteins were purified by amylose affinity and S-300 Sephacryl chromatography. Peak fractions corresponding to a mass of ~130 kDa were incubated with concentrations of EGS from 0.1 mM to 2.5 mM (indicated by the wedge) for 30 min. Cross-linked products were analyzed by SDS-PAGE and Western blotting using an anti-MBP polyclonal antibody and anti-rabbit immunoglobulin conjugated to horseradish peroxidase. Proteins were detected by chemiluminescence. Masses of marker proteins are indicated on the *left*. Positions of the MBP-A22 and MBP-RuvC monomers are indicated by *arrows* in *Panels A* and *B*, respectively.

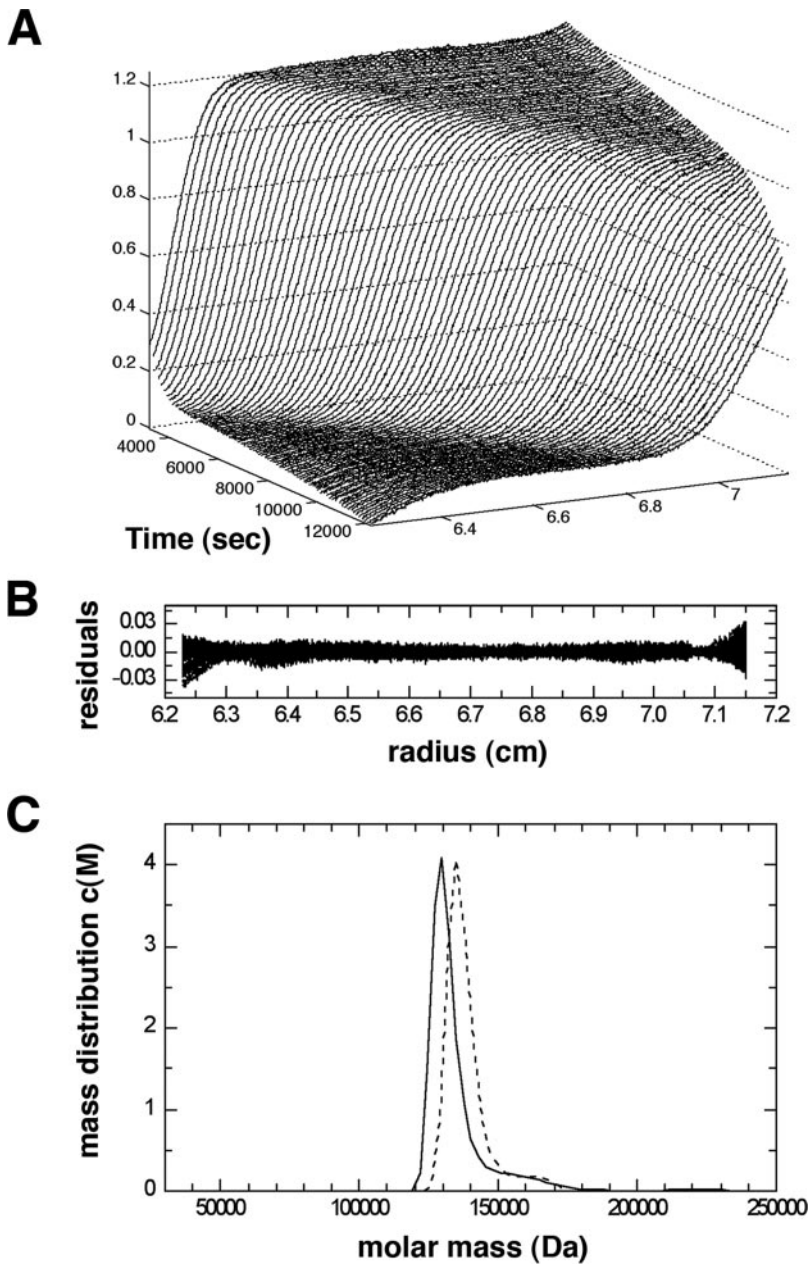

FIGURE 3. **Sedimentation velocity.** *A*, experimental fringe displacement profiles for MBP-A22 obtained at a rotor speed of 50,000 rpm. For clarity, best-fit estimates of the time-invariant and radius-invariant signal contributions were removed. *B*, residuals of the fit (every second scan shown) of a continuous sedimentation coefficient distribution with a best-fit frictional ratio of 1.61. *C*, corresponding molar mass distribution for MBP-A22 (*solid line*) and MBP-RuvC (*dashed line*).

A22 Binds to HJ DNA as a Dimer—We previously used a gel mobility shift assay to demonstrate that A22 can bind to a synthetic HJ (19). Here, we took advantage of the presence of a protease cleavage site between the MBP and A22 domains of the fusion protein to determine whether A22 binds as a monomer or dimer. The method has been used for other HJ resolvases (34, 35) and is based on the predicted differences in the mobilities of short synthetic HJ DNA bound to resolvase monomers and homo- and heterodimers. If partially digested MBP-A22 containing MBP-A22 and A22 species binds to HJ DNA as monomers, then there should be only two complexes *e.g.* A22(HJ) and MBP-A22(HJ). However, if the resolvase binds as a dimer, then there could be three species *e.g.* A22:A22(HJ)), A22:MBP-A22(HJ)), and MBP-A22:MBP-A22(HJ)). Purified recombinant A22, MBP-A22, and MBP-A22 partially digested with proteinase factor Xa were incubated with a synthetic HJ and then analyzed by gel electrophoresis. Predominantly single gel-shifted species migrating rapidly and slowly were obtained with A22 and undigested MBP-A22, respectively (Fig. 5). In contrast, an additional major species with mobility intermediate between that of A22(HJ) and MBP-A22(HJ) was obtained with factor Xa-digested MBP-A22 (Fig. 5). We concluded that A22 exists as a dimer in solution and when bound to DNA.

In addition to the major species described above, there were also minor high molecular weight bands that could result from binding of a second dimer to DNA non-specifically or the interaction of larger multimers with DNA. Uncharacterized high molecular weight bands were previously seen with CCEI and YDC2 (34, 37).

Sequence Cleavage Analysis of A22—Recombinant A22 specifically cleaves four- and three-stranded junctions but does not cleave single- or double-stranded DNA, Y junctions, or branched forms (19). Here we investigated the sequence-specificity of HJ cleavage. When MBP-A22 was digested with proteinase factor Xa to release the A22 moiety, the latter was severely aggregated as previously observed for recombinant A22 protein. Therefore the uncleaved MBP-A22 was used as other studies had shown that N-terminal fusions do not alter the specificities of

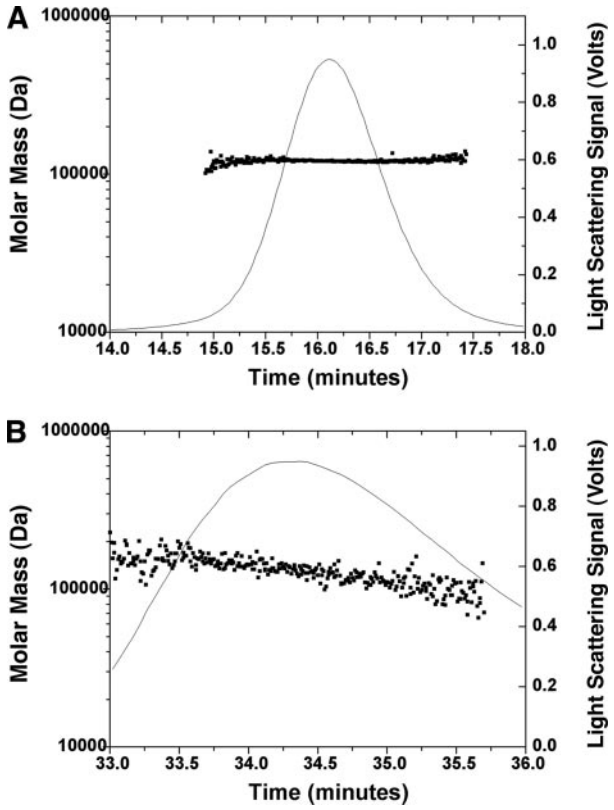

FIGURE 4. **On-line size exclusion chromatography multi-angle laser light scattering.** Molar mass determinations for MBP-RuvC and MBP-A22 are shown in *panels A* and *B*, respectively. For each protein the non-aggregate peak *versus* elution time is shown as a thin line (light scattering signal *right Y axis*) with molar mass values (*left Y axis*) calculated across each respective peak at time intervals of 0.5 s.

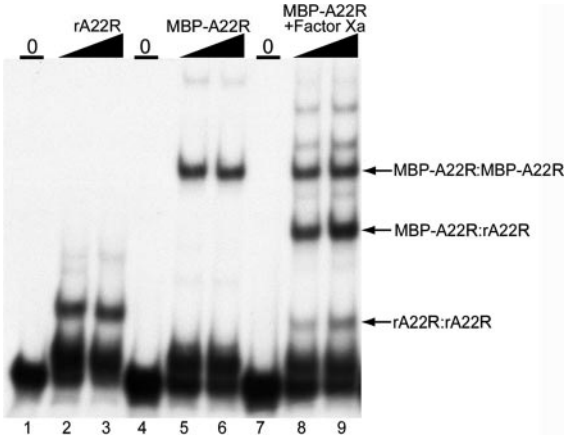

FIGURE 5. **Gel shift mobility assay.** Affinity-purified MBP-A22 was treated with Factor Xa protease to generate a mixture of cleaved and uncleaved fusion proteins. 0, 50, or 100 ng of rA22 (19), MBP-A22, or MBP-A22 digested with Factor Xa were incubated with 0.01 pmol of 5′-^{32}P end-labeled HJ-1 DNA. DNA-protein complexes were analyzed by electrophoresis through a 4% polyacrylamide gel, and bands were visualized by autoradiography. The wedges indicate increasing quantities of fusion proteins in DNA binding reactions. The positions of MBP-A22/MBP-A22 homodimer, MBP-A22/A22 heterodimer, and A22/A22 homodimer complexes are indicated.

RuvC or CCE1 (34, 35). In addition, the MBP-RuvC fusion protein was used as a control. The first synthetic DNA substrate tested, HJ-1, has a short homology region allowing two steps of branch migration. The DNA strands were individually 5′-^{32}P-labeled and four separate complexes were prepared, each labeled on one strand. After incubation with MBP-A22 or MBP-RuvC, cleavage products were separated by denaturing gel electrophoresis next to sequence markers formed by cleavage of

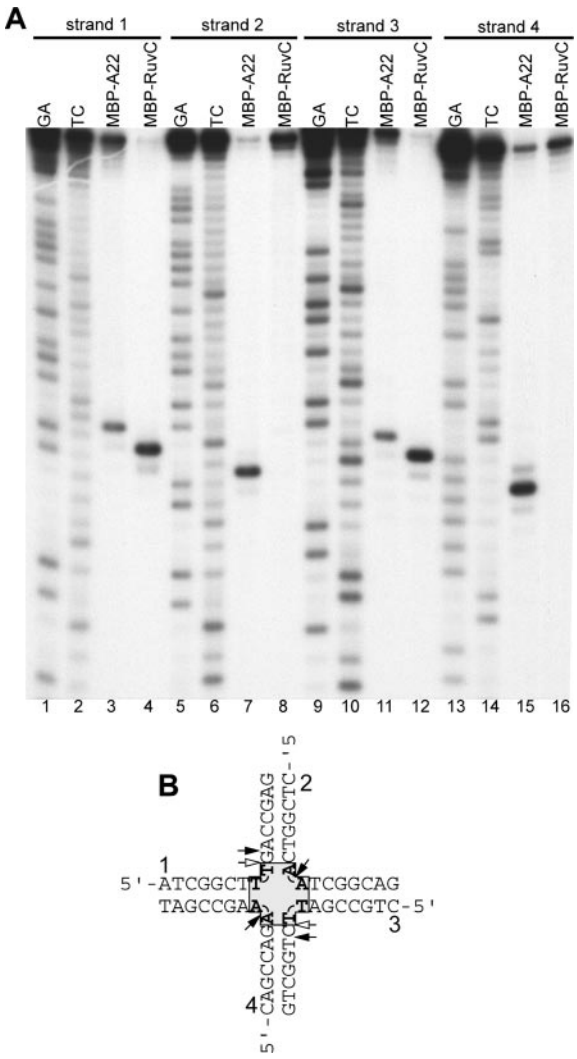

FIGURE 6. **Cleavage of HJ-1 by A22 and RuvC.** *A*, MBP-A22 and MBP-RuvC, purified by affinity chromatography and gel filtration, were incubated with 1 pmol of HJ-1, which was 5′-^{32}P end-labeled on one of the 4 strands as indicated. Following termination and proteinase K digestion, cleavage products were denatured and analyzed by electrophoresis through a 10% polyacrylamide gel next to ^{32}P-labeled sequencing ladders of the same labeled DNA strand (indicated by *GA* and *TC*). Bands were visualized by autoradiography. Cleavage of indicated strands by A22 are shown in *lanes 3*, *7*, *11*, and *15*, and cleavage of indicated strands by RuvC are shown in *lanes 4*, *8*, *12*, and *16*. *B*, central nucleotide sequences of the HJ-1 substrate contain a 2-bp region of homology (shown in the *shaded area*) that permits 2-step branch migration. The positions of A22 and RuvC cleavage sites are indicated by *black arrows* and *white arrows*, respectively.

^{32}P-labeled strands at A+G or C+T nucleotides by formate or hydrazine, respectively. An autoradiograph of a gel is reproduced in Fig. 6*A*. Strong cleavages of A22 occurred symmetrically 3′ to A residues within the homology region of strands 2 and 4 (Fig. 6*B*). Additional cuts occurred just outside of the homology region in strands 1 and 3. In contrast, the major cleavages of RuvC occurred 3′ to T residues on strands 1 and 3 (Fig. 6*B*). Thus, A22 and RuvC have distinctive sequence or structure preferences.

To further analyze the sequence specificity of the A22 resolvase, we used the substrate DNA HJ bm4, which has a homology region with 12 steps of branch migration allowing all possible dinucleotide combinations at the four-way junction (37). Strong cleavages of A22 occurred symmetrically at four sites within the homology region of strands 1 and 3; all but one cleavage occurred 3′ to C residues (Fig. 7, *A* and *B*). However, cleavage occurred next to other residues in strands 2 and 4. In contrast, the major cleavage sites of RuvC occurred after T residues on

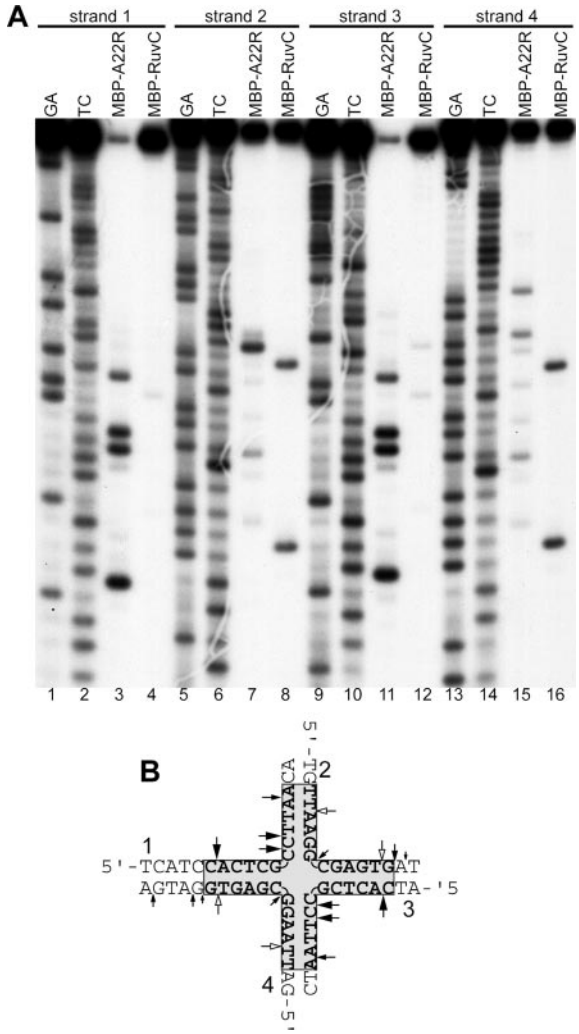

FIGURE 7. **Cleavage of HJ bm4 by A22 and RuvC.** *A*, cleavage reactions were performed and analyzed as described in the legend to Fig. 6 except that the HJ bm4 DNA junction was used as substrate. Cleavage of indicated strands by A22 are shown in *lanes 3*, *7*, *11*, and *15*, and cleavage of indicated strands by RuvC are shown in *lanes 4*, *8*, *12*, and *16*. *B*, nucleotide sequences that comprise the central region of homology of HJ mb4 allowing a 12-step branch migration are shown in the *shaded area*. The *black* and *white arrows* indicate strong cleavage sites of A22 and RuvC, respectively. *Small black arrows* show weaker A22 cleavage sites.

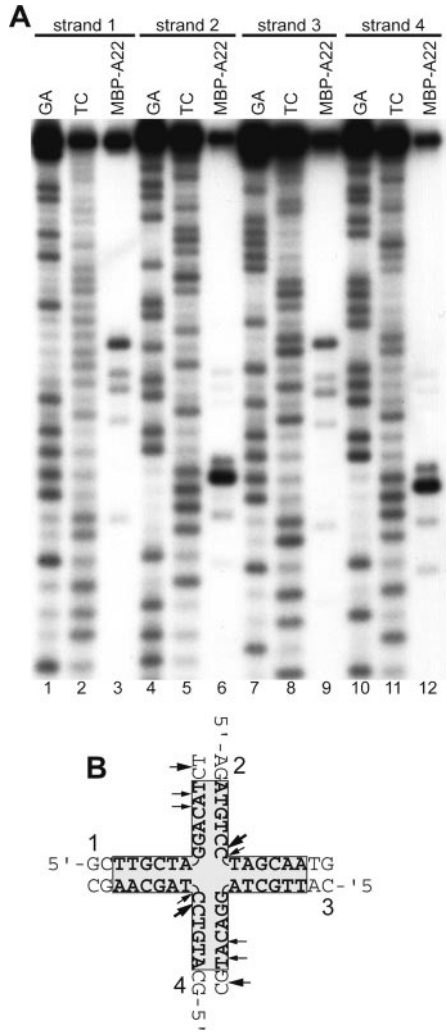

FIGURE 8. **Cleavage of HJ X12 by A22.** *A*, cleavage reactions were performed and analyzed as described in the legend to Fig. 6 except that the HJ X12 DNA junction was used as substrate and only the products of MBP-A22 digestion were analyzed. Cleavage of indicated strands are shown in *lanes 3*, *6*, *9*, and *12*. *B*, nucleotide sequences that comprise the central region of homology allowing a 12-step branch migration are shown in the *shaded area*. *Large* and *small arrows* indicate stronger and weaker cleavages, respectively.

strands 2 and 4 (Fig. 7, *A* and *B*). We also analyzed the sequence preference of A22 using a second 4-strand junction (HJ X12) capable of 12 steps of branch migration (38). Cleavages occurred symmetrically mostly but not exclusively 3′ to C residues (Fig. 8, *A* and *B*). Although A22 appears to prefer cleaving 3′ to C residues in some HJs allowing extensive branch migration, this apparent specificity is far less than that of RuvC for T residues.

Finally, to determine whether strand migration was required for cleavage, we analyzed the fixed four-way junctions Jun3. Cleavages occurred on all four DNA strands either 3′ to the junction or the adjacent nucleotide with no clear sequence specificity (Fig. 9).

DISCUSSION

The dimeric state of RuvC is an important structural feature that allows it to simultaneously and symmetrically cleave homologous strands of a HJ. The severe aggregation of purified recombinant A22, however, prevented studies of its quaternary structure. We overcame the problem by expressing A22 fused to MBP. Previous studies had shown that MBP fusion proteins of RuvC and CCE1 did not affect DNA binding or sequence specificity (34, 35) and this was confirmed for RuvC here. Although the A22 fusion protein also aggregated at 0.2 M NaCl, disaggregation occurred at 0.8 M NaCl indicating the importance of ionic interactions. The dimeric state of disaggregated MBP-A22 was demonstrated by a variety of techniques including gel filtration, chemical cross-linking, sedimentation, and light scattering. Gel mobility shift experiments, carried out in our initial characterization of A22 (19), indicated that despite its extensive aggregation in solution the recombinant protein forms a discrete complex with a synthetic HJ. Presumably, the aggregation state of A22 is dynamic even at low salt and disaggregated species bind specifically to HJs or the DNA directly dissociates aggregates. Here we took advantage of the MBP-A22 fusion protein to prove that the resolvase binds to the HJ as a dimer. After partially cleaving the fusion protein at a specific site between the MBP and A22 domains, the products were incubated with a HJ. Three HJ DNA complexes were resolved, whereas only two could occur if the binding species were monomers. The additional species had a mobility between that of HJ complexes containing A22 alone and undigested MBP-A22 indicating that it contains the hybrid A22:MBP-A22 dimer. As with RuvC, A22

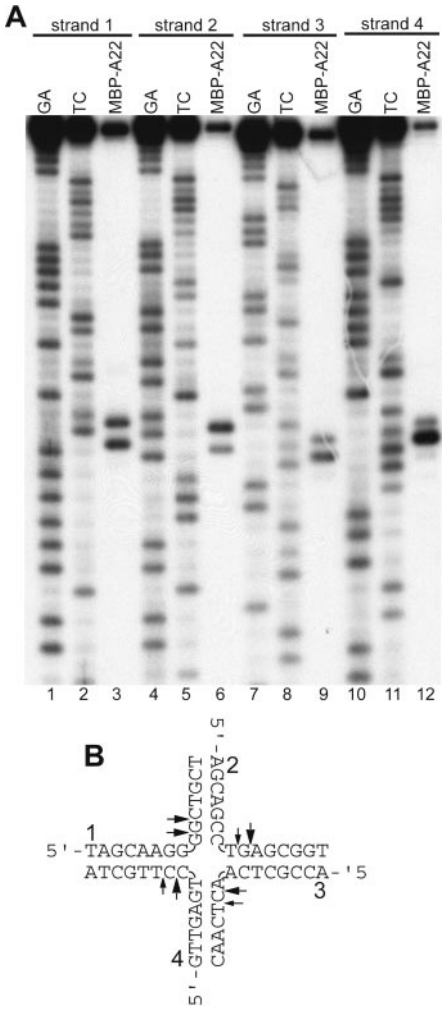

FIGURE 9. **Cleavage of fixed HJ Jun 3 by A22.** *A*, cleavage reactions were performed and analyzed as described in the legend to Fig. 6 except that the HJ Jun 3 DNA junction was used as substrate, and only the products of MBP-A22 digestion were analyzed. Cleavage of indicated strands are shown in *lanes 3*, *6*, *9*, and *12*. *B*, Jun3 substrate consists of oligonucleotides that do not allow branch migration. *Large* and *small arrows* indicate stronger and weaker cleavages, respectively.

dimers would facilitate the simultaneous cleavage of homologous DNA strands.

E. coli RuvC and yeast CCE1 preferentially cleave nucleotide sequences with the consensus 5-(A/T)TT ↓ (G/C)-3′ (24, 25) and 5′-ACT ↓ A (39), respectively, at or within one or two nucleotides of the point of strand exchange. Presumably, sequence specificity helps to ensure that cleavage occurs at homologous sites during recombination. Several HJs were synthesized to investigate the sequence and structural specificity of A22. Using two different HJs with long homology regions allowing extensive branch migration, we found that paired cuts often occurred 3′ of C residues, though cuts occurred after other nucleotides as well. This apparent preference by A22 for C residues was much less than that of RuvC for T residues and could have explanations other than recognition of a primary sequence. Indeed, the absence of a sequence requirement by A22 was clearly demonstrated using HJs that lacked C residues in the homology regions. With a fixed HJ unable to undergo branch migration, A22 cleaved 3′ of A or T residues in preference to more distal C residues. Clearly, the HJ structure is essential whereas homologous or preferred sequences are not. Thus, with regard to sequence specificity, A22 differs from RuvC and CCE1.

Previous studies indicated that A22 expression is required for resolution of DNA concatemers (19, 20). However, the apparent lack of cleavage sequence specificity of A22 contrasts with the well defined DNA sequence requirements for resolution of poxvirus DNA concatemers (40–42). It is possible that a cleavage sequence preference occurs *in vivo* under conditions in which branch migration allows extensive sampling of target poxvirus DNA. However, it is more likely that additional viral proteins are involved in determining the site of resolution. In *E. coli*, RuvC forms part of a resolvase complex with RuvA and RuvB, which are required for branch migration (37). However, no homologs of RuvA or RuvB are present in poxviruses. There is a remarkable similarity between the concatemer junction sequence and a viral late promoter leading to the interesting suggestion that the transcription initiation complex may unwind the double helix allowing formation of the HJ structure (43, 44). Perhaps by collaborating with the transcription complex, the structural specificity of A22 ensures that cleavage occurs at the proper site. In this regard, we have shown using a supercoiled plasmid that A22 specifically cleaves within the palindromic concatemer junction.[5]

The packaged genomes of VACV contain no nicks (45, 46). Consequently, if the A22 protein resolves concatemers *in vivo*, as suggested by a previous study (21), the nicks must be sealed. VACV does encode a DNA ligase; however, it not essential for virus replication in tissue culture cells (47–50). There is a possibility that a cellular ligase complements DNA ligase deletion mutants and seals nicks formed by the A22 protein, though the cellular enzyme would need to do this within viral factory areas in the cytoplasm. Alternatively, the cleaved DNA may not be sealed in the absence of the viral DNA ligase; perhaps the genomes of DNA ligase deletion mutants contain near terminal nicks that do not abrogate infectivity.

The structural and functional similarity between poxvirus, bacterial and yeast mitochondrial HJ resolvases, support their common evolution as originally predicted from sequence analysis. The absence of a related resolvase in mammals suggests that these microbial proteins might represent specific drug targets.

REFERENCES

1. Moss, B. (1996) in *Poxviridae*: *The Viruses and Their Replication*, *Fields Virology* (Fields, B. N., Knipe, D. M., and Howley, P. M., eds) 3rd Ed., pp. 2637–2671, Lippincott-Raven Publishers, Philadelphia
2. Baroudy, B. M., Venkatesan, S., and Moss, B. (1982) *Cell* **28,** 315–324
3. Moyer, R. W., and Graves, R. L. (1981) *Cell* **27,** 391–401
4. Baroudy, B. M., Venkatesan, S., and Moss, B. (1982) *Cold Spring Harbor Symp. Quant. Biol.* **47,** 723–729
5. Delange, A. M., Reddy, M., Scraba, D., Upton, C., and McFadden, G. (1986) *J. Virol.* **59,** 249–259
6. Merchlinsky, M., and Moss, B. (1986) *Cell* **45,** 879–884
7. Merchlinsky, M. (1990) *J. Virol.* **64,** 3437–3446
8. Dickie, P., Morgan, A. R., and McFadden, G. (1987) *J. Mol. Biol.* **196,** 541–558
9. Merchlinsky, M., Garon, C., and Moss, B. (1988) *J. Mol. Biol.* **199,** 399–413
10. Sharples, G. J. (2001) *Mol. Microbiol.* **39,** 823–834
11. DeLange, A. M. (1989) *J. Virol.* **63,** 2437–2444
12. Merchlinsky, M., and Moss, B. (1989) *J. Virol.* **63,** 1595–1603
13. Stuart, D., Ellison, K., Graham, K., and McFadden, G. (1992) *J. Virol.* **66,** 1551–1563
14. Shaffer, R., and Traktman, P. (1987) *J. Biol. Chem.* **262,** 9309–9315
15. Shuman, S., and Moss, B. (1987) *Proc. Natl. Acad. Sci. U. S. A.* **84,** 7478–7482
16. Palaniyar, N., Gerasimopoulos, E., and Evans, D. H. (1999) *J. Mol. Biol.* **287,** 9–20
17. Sekiguchi, J., Seeman, N. C., and Shuman, S. (1996) *Proc. Natl. Acad. Sci. U. S. A.* **93,** 785–789
18. Da Fonseca, F., and Moss, B. (2003) *Proc. Natl. Acad. Sci. U. S. A.* **100,** 11291–11296
19. Garcia, A. D., Aravind, L., Koonin, E. V., and Moss, B. (2000) *Proc. Natl. Acad. Sci. U. S. A.* **97,** 8926–8931
20. Aravind, L., Makarova, K. S., and Koonin, E. V. (2000) *Nucleic Acids Res.* **28,** 3417–3432
21. Garcia, A. D., and Moss, B. (2001) *J. Virol.* **75,** 6460–6471

[5] A. D. Garcia, unpublished data.

22. Iwasaki, H., Takahagi, M., Shiba, T., Nakata, A., and Shinagawa, H. (1991) *EMBO J.* **10,** 4381–4389
23. Ariyoshi, M., Vassylyev, D. G., Iwasaki, H., Nakamura, H., Shinagawa, H., and Morikawa, K. (1994) *Cell* **78,** 1063–1072
24. Shah, R., Bennett, R. J., and West, S. C. (1994) *Cell* **79,** 853–864
25. Eggleston, A. K., and West, S. C. (2000) *J. Biol. Chem.* **275,** 26467–26476
26. Schuck, P. (2000) *Biophys. J.* **78,** 1606–1619
27. Schuck, P., and Demeler, B. (1999) *Biophys. J.* **76,** 2288–2296
28. Schuck, P., Perugini, M. A., Gonzales, N. R., Howlett, G. J., and Schubert, D. (2002) *Biophys. J.* **82,** 1096–1111
29. Wen, J., Arakawa, T., and Philo, J. S. (1996) *Anal. Biochem.* **240,** 155–166
30. Saito, A., Iwasaki, H., Ariyoshi, M., Morikawa, K., and Shinagawa, H. (1995) *Proc. Natl. Acad. Sci. U. S. A.* **92,** 7470–7474
31. Giraud-Panis, M. J., and Lilley, D. M. (1998) *J. Mol. Biol.* **278,** 117–133
32. Lloyd, R. G., and Sharples, G. J. (1993) *Nucleic Acids Res.* **21,** 1719–1725
33. Maxam, A. M., and Gilbert, W. (1977) *Proc. Natl. Acad. Sci. U. S. A.* **74,** 560–564
34. White, M. F., and Lilley, D. M. (1996) *J. Mol. Biol.* **257,** 330–341
35. Shah, R., Cosstick, R., and West, S. C. (1997) *EMBO J.* **16,** 1464–1472
36. Siegel, L. M., and Monty, K. J. (1966) *Biochim. Biophys. Acta* **112,** 346–362
37. White, M. F., and Lilley, D. M. (1997) *Mol. Cell. Biol.* **17,** 6465–6471
38. Parsons, C. A., and West, S. C. (1993) *J. Mol. Biol.* **232,** 397–405
39. Schofield, M. J., Lilley, D. M., and White, M. F. (1998) *Biochemistry* **37,** 7733–7740
40. DeLange, A. M., and McFadden, G. (1987) *J. Virol.* **61,** 1957–1963
41. Merchlinsky, M., and Moss, B. (1989) *J. Virol.* **63,** 4354–4361
42. Merchlinsky, M. (1990) *J. Virol.* **64,** 5029–5035
43. Hu, F.-Q., and Pickup, D. J. (1991) *Virology* **181,** 716–720
44. Stuart, D., Graham, K., Schreiber, M., Macaulay, C., and McFadden, G. (1991) *J. Virol.* **65,** 61–70
45. Geshelin, P., and Berns, K. I. (1974) *J. Mol. Biol.* **88,** 785–796
46. Garon, C. F., Barbosa, E., and Moss, B. (1978) *Proc. Natl. Acad. Sci. U. S. A.* **75,** 4863–4867
47. Colinas, R. J., Goebel, S. J., Davis, S. W., Johnson, G. P., Norton, E. K., and Paoletti, E. (1990) *Virology* **179,** 267–275
48. Kerr, S. M., and Smith, G. L. (1989) *Nucleic Acids Res.* **17,** 9039–9050
49. Kerr, S. M., and Smith, G. L. (1991) *Virology* **180,** 625–632
50. Kerr, S. M., Johnston, L. H., Odell, M., Duncan, S. A., Law, K. M., and Smith, G. L. (1991) *EMBO J.* **10,** 4343–4350